Characterization of a lamprophyre facies unit hosted in Timiskaming Group metasedimentary rocks: implications for subsidiary structures of the Cadillac-Larder Lake Deformation Zone, Quebec

A.M. BRADLEY, T.R.C. JØRGENSEN, and P.C. THURSTON

Mineral Exploration Research Centre, Harquail School of Earth Sciences, Goodman School of Mines, Laurentian University, 935 Ramsey Lake Rd., Sudbury, ON, P3E 2C6, Canada

LaurentianUniversity UniversitéLaurentienne
HARQUAIL SCHOOL OF EARTH SCIENCES ÉCOLE DES SCIENCES DE LA TERRE
METAL EARTH
MERC Mineral Exploration Research Centre
GOODMAN SCHOOL OF MINES ÉCOLE DES MINES
CANADA FIRST RESEARCH EXCELLENCE FUND
APOGÉE CANADA FONDS D'EXCELLENCE EN RECHERCHE

INTRODUCTION

This study focuses on the petrogenesis of an enriched Mg-Cr-Ni unit ~300 m south of the Cadillac-Larder Lake Deformation Zone (CLLDZ) in order to determine if it is part of the Timiskaming Group metasedimentary host rocks, a syn-sedimentary volcanic unit, a structurally emplaced part of the Piché Structural Complex (PSC), a late but pre- to syn-deformation intrusive rock, and its implications for mineralization. Detailed mapping, petrography and whole-rock geochemistry, suggest that it is a lamprophyre facies unit that potentially represents a subsidiary structure of the CLLDZ.

GEOLOGICAL SETTING OF STUDY AREA

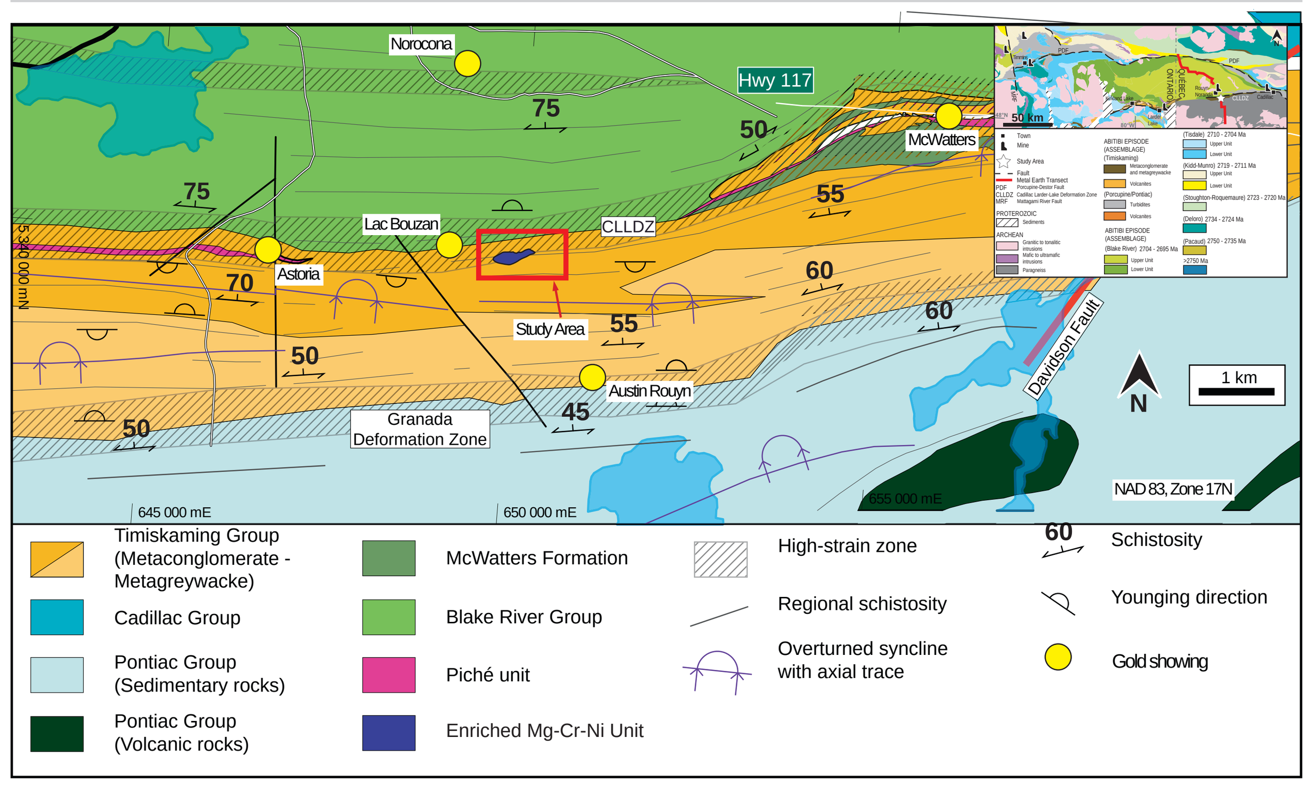

Figure 1. Geological map of the CLLDZ in the Rouyn-Noranda segment (after Bedeaux et al., 2017). Red box is the study area, enlarged in Figure 2. Insert displays the regional setting (modified after Thurston et al., 2008). Universal Transverse Mercator (UTM) coordinates in NAD83, Zone 17N.

The CLLDZ is an east-trending, steeply dipping, trans-crustal deformation zone with intense carbonate alteration, high strain, and orogenic style quartz-carbonate-Au mineralization (Bedeaux et al., 2017). The CLLDZ is interpreted as a primary hydrothermal pathway, however, significant mineralized quartz veins are commonly hosted in subsidiary structures (Bedeaux, 2018). The CLLDZ includes metavolcanic rocks of the ca. 2709 Ma PSC (David et al., 2018), 2704-2695 Ma Blake River Group (Thurston et al., 2008), metasedimentary rocks of the ca. 2682 Ma Pontiac Group (Frieman et al., 2017), and the 2679-2669 Ma Timiskaming Group (Frieman et al., 2017). The enriched Mg-Cr-Ni unit lies ~3 km south of Rouyn-Noranda and ~300 m south of the CLLDZ within the Granada Formation (Wilson, 1962; Dimroth et al., 1982). Wilson (1962) mapped the enriched Mg-Cr-Ni unit as an amphibole schist in the Pontiac Group, implying an intrusive or structural emplacement. Alternatively, Diop (2011) described the unit as a mafic volcanoclastic sandstone of the Timiskaming Group.

DETAILED MAPPING AND SAMPLE LOCATIONS

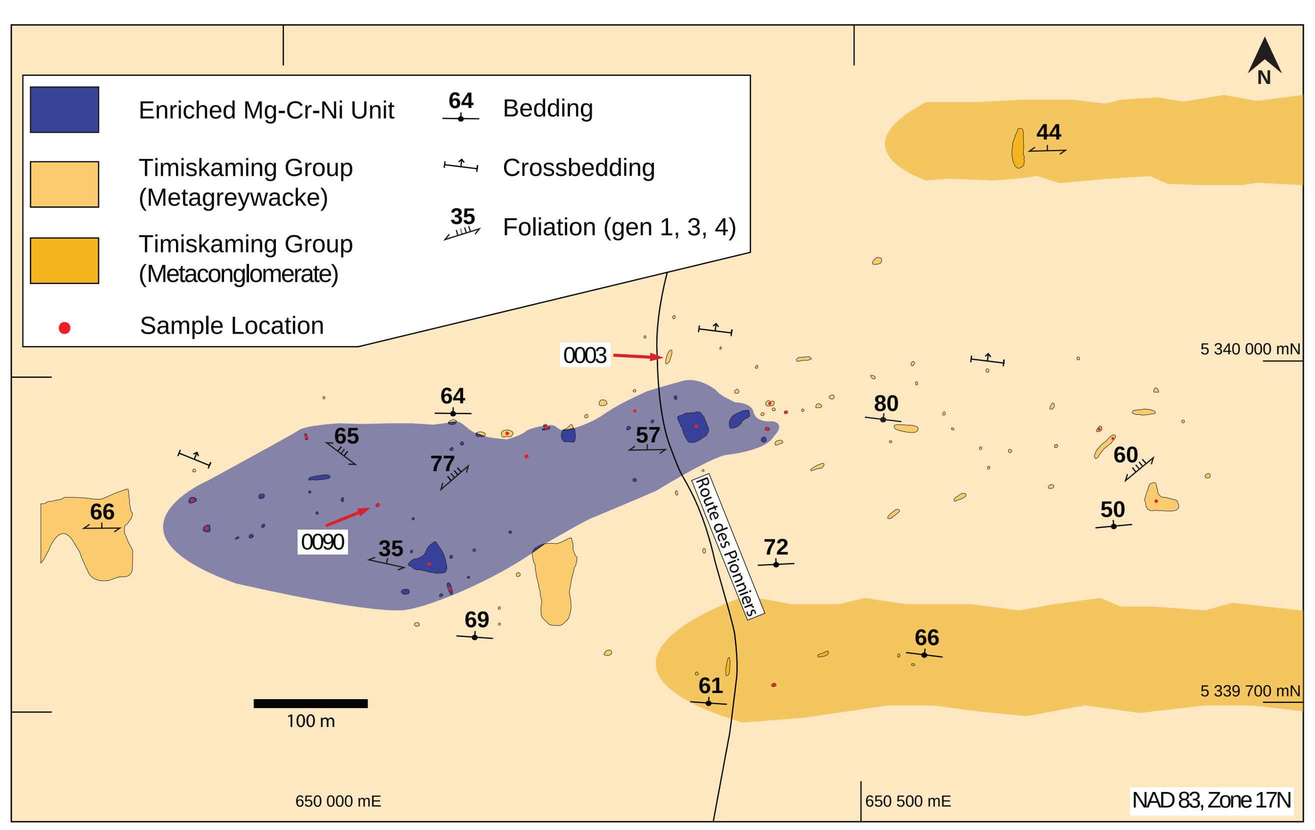

Figure 2. Detailed geological map showing the distribution of the enriched Mg-Cr-Ni unit. UTM coordinates in NAD83, Zone 17N.

Field mapping at 1:1000 scale delimited four units: 1) an enriched Mg-Cr-Ni unit (dark blue colour in Fig. 2) characterized by a melanocratic, chlorite ± talc matrix and 1-15 modal%, 1-4 mm amphibole and biotite; 2) a metagreywacke characterized by a meso to melanocratic, grey, and biotite-quartz ± plagioclase beds. Locally, intercalated conglomerate beds (< 1 m thickness) contain flattened mafic clasts and 1-2% granitic clasts similar to those in the Timiskaming metaconglomerate; 3) a polymictic metaconglomerate characterized by a mesocratic, grey, fine to medium-grained matrix and ~50-60 modal%, 2-15 cm granitic clasts and; 4) a magnetite-bearing polymictic metaconglomerate distinguished by ~1 mm, euhedral, magnetite cubes throughout the matrix. The nature of the contact is sharp and regular on the cm-scale, and irregular on the outcrop scale.

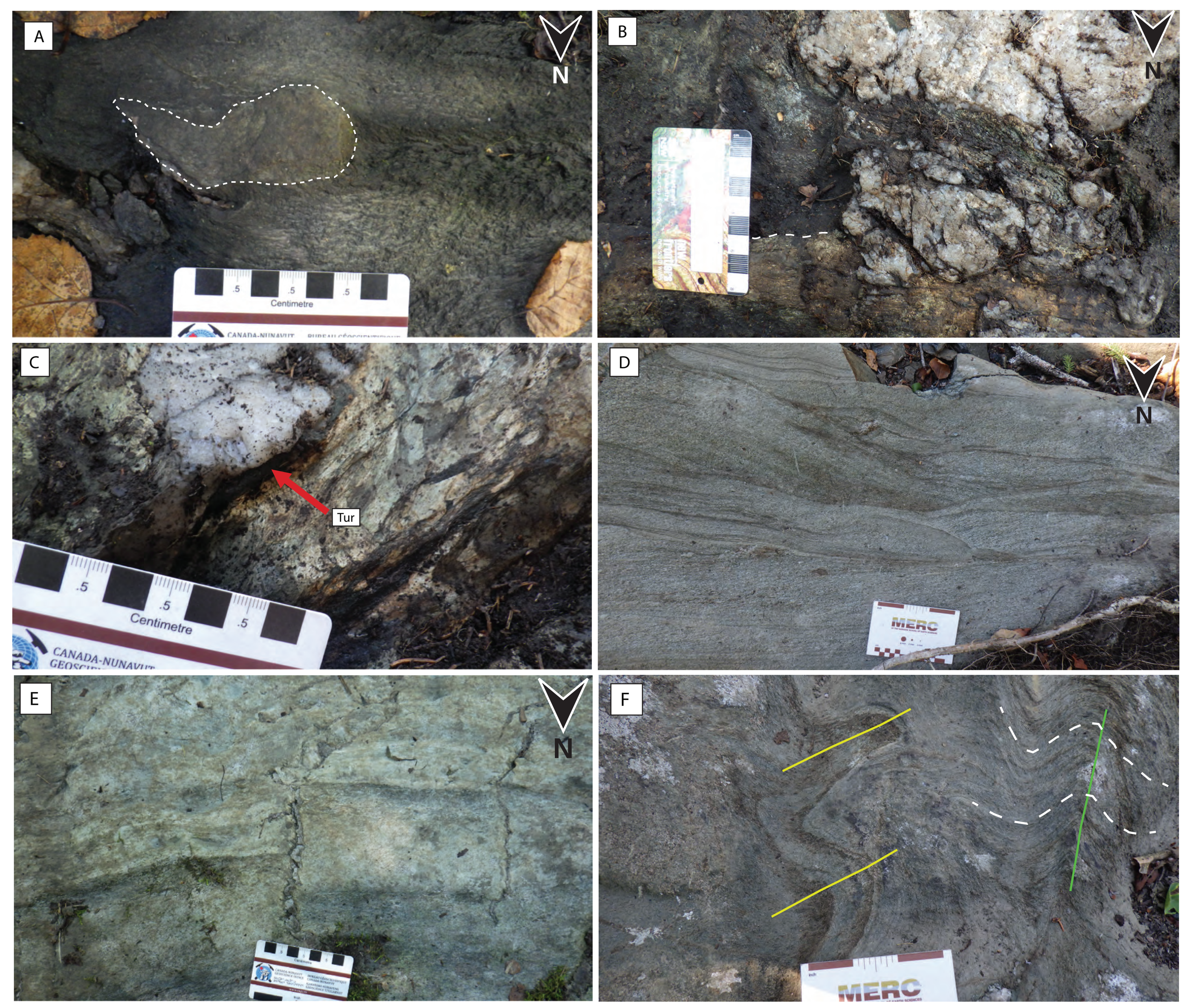

Figure 3. A) Rounded clast (white dashed line) in the enriched Mg-Cr-Ni unit. Note melanocratic dark green colour and distinct crenulation cleavage. B) A deformed quartz-carbonate vein exploits the sharp northern contact between the enriched Mg-Cr-Ni unit (top) and Timiskaming metagreywacke (bottom). C) Quartz-tourmaline vein in host Timiskaming metagreywacke < 1 m from the contact of the enriched Mg-Cr-Ni unit. D) Trough cross-bedded host Timiskaming metagreywacke. E) Offset bedding in the Timiskaming metagreywacke. F) Early folds (yellow lines are axial plane traces) overprinted by later folds associated with a strong crenulation cleavage (green line) in the enriched Mg-Cr-Ni unit ~1 m from the northern contact with the Timiskaming metagreywacke.

PETROGRAPHY

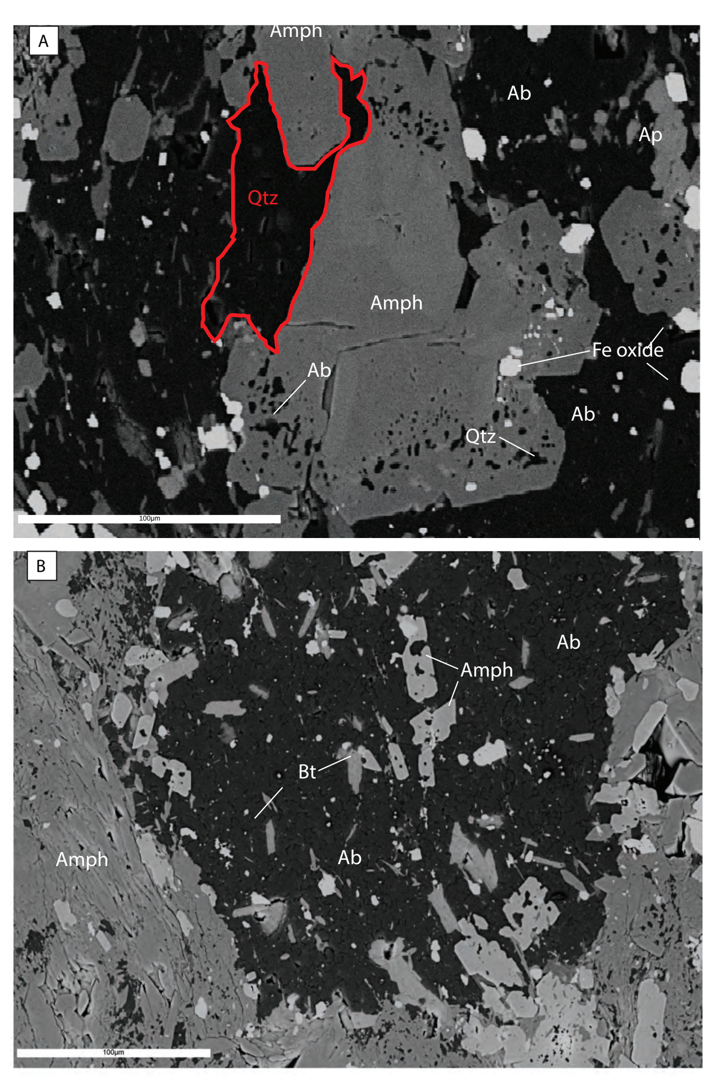

Locally, the enriched Mg-Cr-Ni unit shows a glomerophyric texture of amphibole phenocrysts (Fig. 4A). Individual amphibole grains are generally euhedral to subhedral. Parts of some amphibole grains contain a significant amount of quartz, iron oxide, and plagioclase inclusions, which probably represent partial overprinting by low grade metamorphism. All plagioclase grains analyzed by semi-quantitative scanning electron microscope (SEM) were An<10 and therefore classified as albite. Thus, no primary igneous plagioclase is preserved. It is currently uncertain whether the amphibole grains experienced post-emplacement modification or if they are pristine in nature. Biotite occurs as euhedral to subhedral microphenocrysts along with amphibole in a plagioclase matrix (Fig. 4B).

Figure 4. A) Back scattered electron (BSE) image of an amphibole phenocryst surrounded by amphibole overgrowth with inclusions. Quartz outlined in red is usually only present in trace amounts. B) BSE image showing albite in the groundmass together with eu- to subhedral amphibole and biotite.

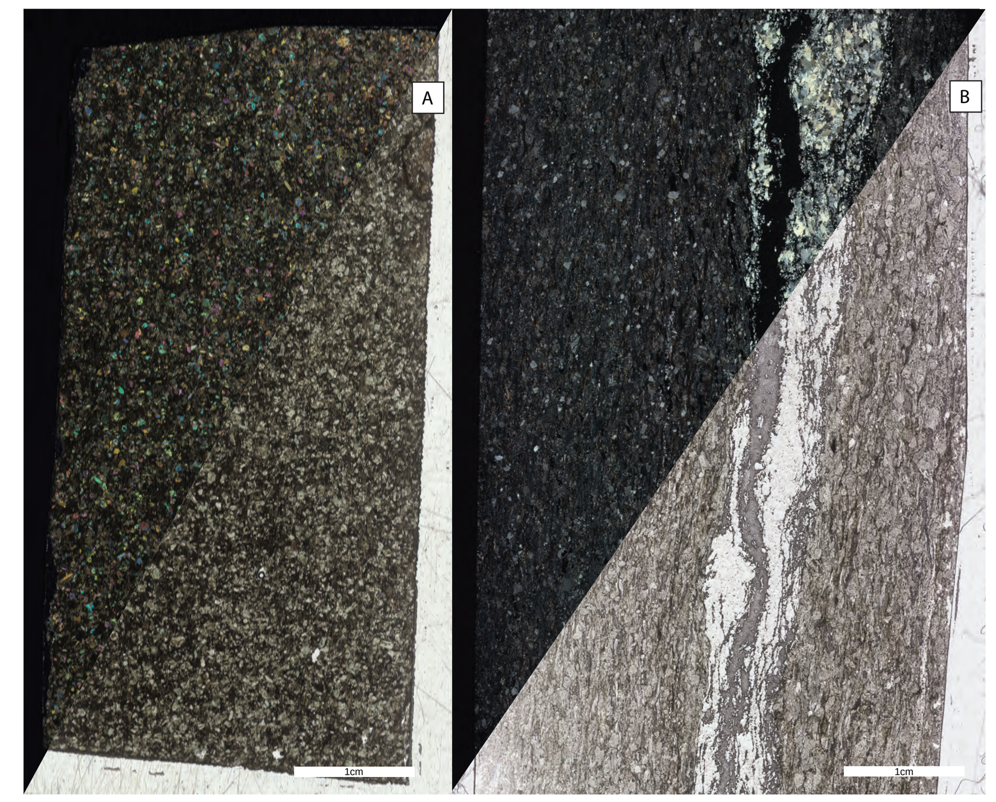

The enriched Mg-Cr-Ni unit largely consists of amphibole, chlorite, biotite, and plagioclase with minor ilmenite, epidote, talc, apatite, and quartz. Accessory phases include titanite, chromite, and zircon. The Timiskaming metagreywacke consists of quartz, plagioclase, and biotite with accessory amphibole.

Figure 5. Plane- and cross-polarized light thin section scans of: A) the enriched Mg-Cr-Ni unit (station 0090), and B) Timiskaming metagreywacke (station 0003). Station locations in Figure 2.

STRUCTURAL ANALYSIS

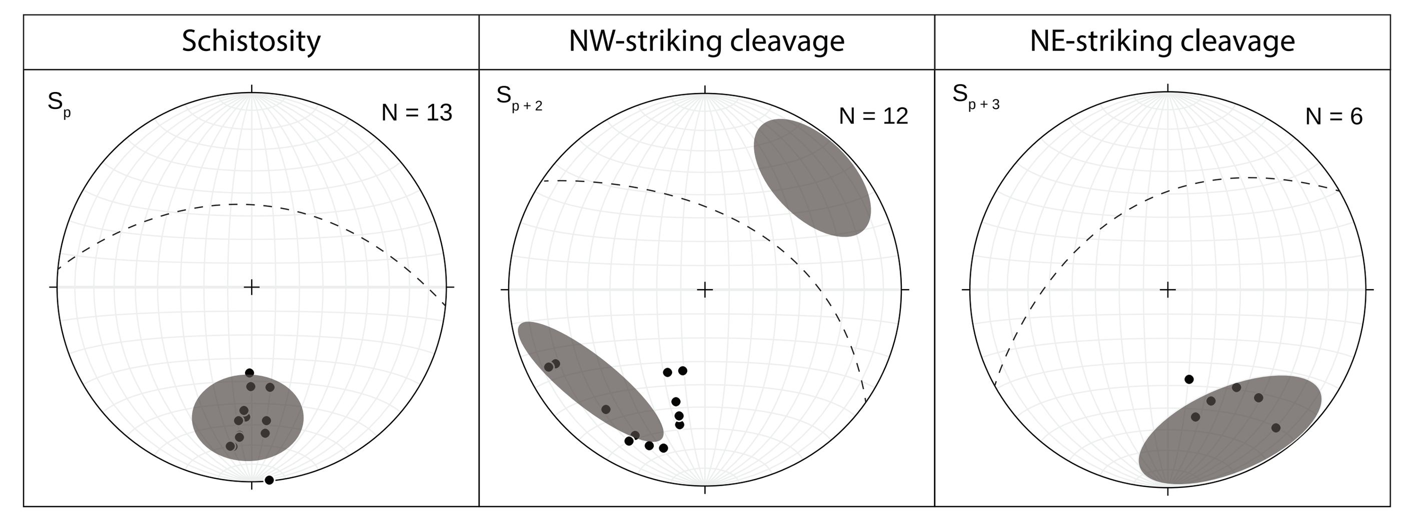

Figure 6. Structural measurements from the study area plotted on stereonets. Grey areas denote data from the Rouyn-Noranda segment of the CLLDZ (Bedeaux et al. 2017) plots for comparison. Plots were produced with Stereonet version 10.

Deformation Event	Bedding and Schistosity Orientation: Bedeaux et al., 2017	Bedding and Schistosity Orientation: This study	Fabric-recording Lithology	Defined by
S_0	E-striking, subvertically N-dipping	E-striking, subvertically N-dipping	Metagreywacke Metaconglomerate	Modal wt.% of Bi, Qtz, and Pl
S_p N-S shortening	E-trending, moderately N-dipping	E-trending, moderately N-dipping	Enriched Mg-Cr-Ni unit Metagreywacke Metaconglomerate	Chl, Amph Bt, elongate Qtz fragments
S_{p+1} extension	Horizontal cleavage	*Not observed*	*Not observed*	Sigmoid and bookshelf objects
S_{p+2} NE-SW shortening	NW-trending, subvertically NE-dipping	NW-trending, steeply NE-dipping	Enriched Mg-Cr-Ni unit	Chl, Amph
S_{p+3} NW-SE shortening	NE-trending, vertically NW-dipping	NE-trending, subvertically NW-dipping	Enriched Mg-Cr-Ni unit	Chl, Amph

Figure 7. Deformation events along the Noranda segment of the CLLDZ and associated structural fabrics, (Bedeaux et al. 2017). This information is compared to observations in the study area. Note that the strong NW-trending, shallowly NE-dipping crenulation cleavage observed in the enriched Mg-Cr-Ni unit is restricted to the contact zone.

WHOLE-ROCK GEOCHEMISTRY

C1 Chondrite normalized (cn) multi-element diagrams of the enriched Mg-Cr-Ni unit and Timiskaming metagreywacke show significant overlap and largely similar patterns (Fig. 8A-C). The samples are enriched in incompatible elements such as Th and the light rare earth elements (LREE) compared to C1 Chondrite (La_{cn} = 31-111). They are also characterized by fractionated REE patterns ($[La/Yb]_{cn} \approx 7.1$), relatively flat heavy REE (HREE) profiles ($[Gd/Lu]_{cn} \approx 2.5$), and strongly negative Nb-Ta-Ti anomalies relative to neighbouring elements. A noticeable difference is the positive Zr-Hf anomaly observed in the metagreywackes, but not in the enriched Mg-Cr-Ni unit. Bivariate plots of MgO vs. SiO_2, Ni, and Cr show a continuous range and approximate linear correlation rather than isolated clusters, with the Timiskaming metagreywackes generally plotting at higher SiO_2 and lower Ni and Cr for a given MgO value (Fig. 8D-F). Only one sample of the enriched Mg-Cr-Ni unit has an MgO content consistent with ultramafic rocks (>18 wt.% MgO). The PSC in the Rouyn-Noranda area is dominated by ultramafic volcanic rocks with flat REE patterns ($[La/Yb]_{\text{Primitive Mantle Normalized}}$ = 1.7; Bedeaux et al., 2018), much different from the REE profiles of the enriched Mg-Cr-Ni unit.

Furthermore, the PSC mafic to intermediate rocks have much lower average concentrations of Cr_2O_3 = 0.0 wt.% and K_2O = 0.4 wt.% (Bedeaux et al., 2018) than the enriched Mg-Cr-Ni unit (Cr_2O_3 = 0.13 wt.%; K_2O = 2.52 wt.%).

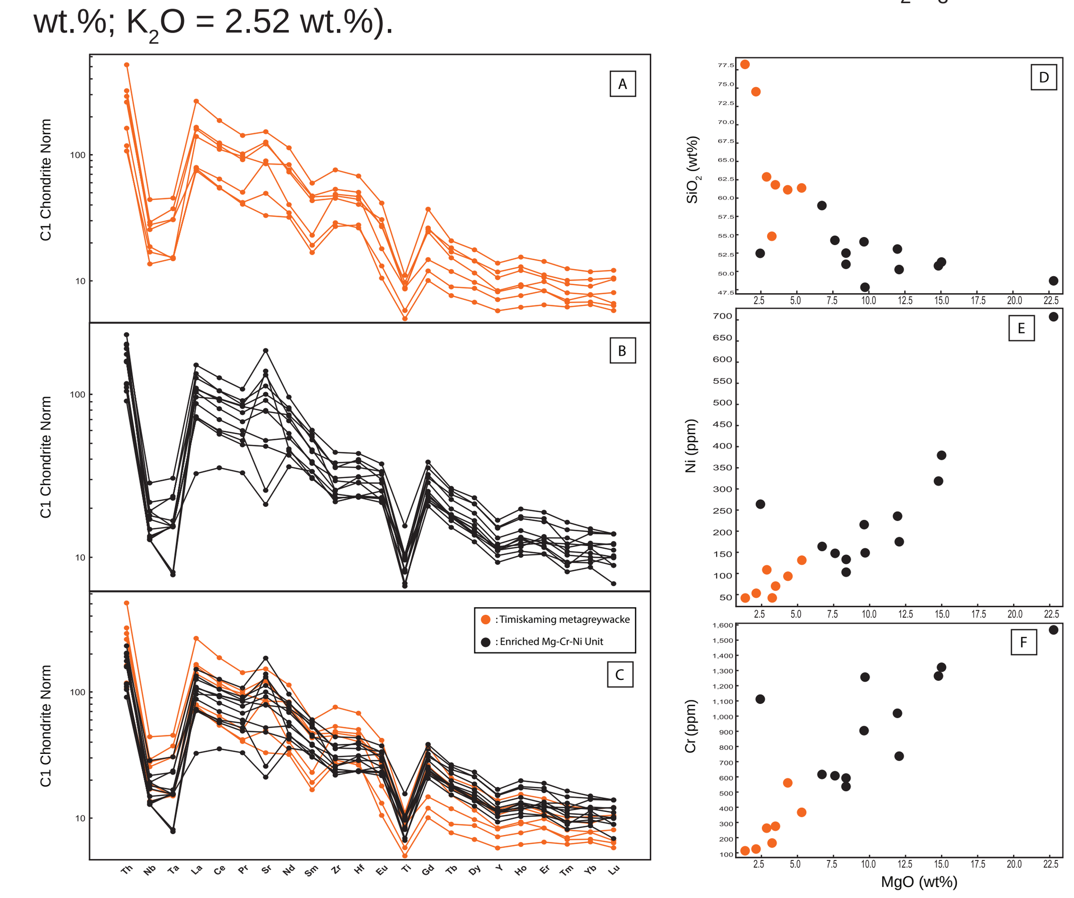

Figure 8. C1 Chondrite normalized multi-element diagrams (McDonough and Sun, 1995) (A-C) and bivariate plots of MgO versus Cr (D), Ni (E), and SiO_2 (F).

CONCLUSIONS AND FUTURE WORK

1. Detailed mapping delimited an enriched Mg-Cr-Ni unit within the Timiskaming metagreywackes and metaconglomerates of the Granada Formation. The geochemistry of the enriched Mg-Cr-Ni unit does not match the PSC rocks in the Rouyn-Noranda area. Thus, the enriched Mg-Cr-Ni unit is unlikely to represent a sliver of the PSC south of main CLLDZ. The nature of the contact relationships (sharp, regular), locally preserved igneous textures, the presence of what is interpreted as amphibole phenocrysts and biotite microphenocrysts and a feldspar-bearing matrix is consistent with the enriched Mg-Cr-Ni unit representing a lamprophyre facies unit.

2. The lamprophyre facies unit records the same major deformation events as seen in the Rouyn-Noranda segment of the CLLDZ. Strain partitioning probably explains the generally more deformed nature of the lamprophyre facies unit relative to the host metagreywackes and metaconglomerates. As such, the lamprophyre facies unit delineates a high strain zone in the Granada Formation that is oriented subparallel to the main CLLDZ and shares a similar deformation history.

3. Quartz-tourmaline veins locally occur in the host metagreywacke along the northern contact with the lamprophyre facies unit. These styles of alteration and veining are also commonly associated with the CLLDZ.

4. Based on the above observations and interpretations, it is proposed that the lamprophyre facies unit was emplaced as a dike or a plug. The more intense deformation, structural elements, alteration, and vein types are all features associated with the CLLDZ and as such, the lamprophyre facies unit potentially represents a subsidiary structure of the CLLDZ.

Contact Information

abradley@laurentian.ca; trc.joergensen@gmail.com; pthurston@laurentian.ca

References

Beduaux, P. 2018. ÉVOLUTION STRUCTURALE, MODÉLISATION DES PALÉOCONTRAINTES ET IMPLICATIONS SUR LES MINÉRALISATIONS AURIFÈRES OROGÉNIQUES LE LONG DE FAILLES MAJEURES: APPLICATION À LA FAILLE DE CADILLAC, ABITIBI, CANADA. Unpublished PhD Thesis. Université du Québec à Chicoutimi, Canada.

Bedeaux, P., Mathieu, L., Pilote, P., Rafini, S., and Daigneault, R., 2018. Origin of the Piché Structural Complex and implications for the early evolution of the Archean crustal-scale Cadillac–Larder Lake Fault Zone, Canada. *Can. J. Earth Sci*, **55**. pp. 905-922.

Bedeaux, P., Pilote, P., Diagneault, R., Rafini, S. 2011. Synthesis of the structural evolution and associated gold minerlaization of the Cadillac Fault, Abitibi, Canada. *Ore Geology Reviews*, **82**. pp. 49-69.

David, J., Pilote, P., Hammouche, H., Leclerc, F., Takam, F.T. 2018. Datations U-Pb dans la Province du Supérieur effectuées au GEOTOP en 2014-2018. Quebec, RP 2017-03.

Dimroth, E., Imreh, L., Rocheleau, M., and Goulet, N., 1982. Evolution of the south-central part of the Archean Abitibi Belt, Quebec. Part I: Stratigraphy and paleogeographic model. *Canadian Journal of Earth Sciences*, **19**. pp. 1729-1758.

Diop, A., 2011. Caractéristiques sédimentologiques, volcanologiques et structurales du bassin de Granada dans la ceinture de roches vertes de l'Abitibi (Québec). Unpublished PhD thesis. Université du Québec à Chicoutimi, Canada.

Frieman, B.M., Kuiper, Y.D., Kelly, N.M., Monecke, T., Kylander-Clark, A. 2017. Constraints on the geodynamic evolution of the southern Superior Prov-ince: U-Pb LA-ICP-MS analysis of detrital zircon in successor basins of the Archean Abitibi and Pontiac subprovinces of Ontario and Quebec, Canada. *Precambrian Research*, 292, pp. 398-416.

Mathieu, L., Bouchard, É., Guay, F., Liénard, A., Pilote, P., Goutier, J. 2018. Criteria for the recognition of Archean calc-alkaline lam pro-phyres: examples from the Abitibi Subprovince. *Canadian Journal of Earth Sciences*, **55**. pp. 188-205.

Thurston, P., Ayer, J. A., Goutier, J., and Hamilton, M. A., 2008. Depositional gaps in Abitibi greenstonebelt stratigraphy: a key to explo-ration for syngenetic mineralization. *Economic Geology*, **103**, pp. 1097–1134.

Wilson, M.E. (Geology), 1962. Geology of the South East Rouyn Township in Quebec. *Geological Survey of Canada*, scale 1:1500. 1 sheet.